Determination of Load Dependent Thermal Conductivity of Porous Adsorbents

Kraft[1], Gaiser[1], Stripf[1], Hesse[2]
[1] University of Applied Sciences Karlsruhe, Baden-Württemberg, Germany
[2] TU Dresden

Abstract: Standard measuring techniques for thermal conductivity cannot be readily applied to determine the load-dependent thermal conductivity of porous adsorbents, because the local ad- and desorption inside the specimen is not considered. Hence, in this work a new measuring procedure combining the transient hot bridge (THB) technique with a finite element model set up in COMSOL Multiphysics software for post-processing is presented. An easy to use COMSOL application is developed to determine the load-dependent thermal conductivity considering the local ad- and desorption processes and the specimen geometry. The results of this new procedure can be used for detailed system simulation of ad- and desorption processes, e.g. regenerative filters or adsorption heat pumps.

Keywords: Transient Hot Bridge, thermal conductivity, adsorption

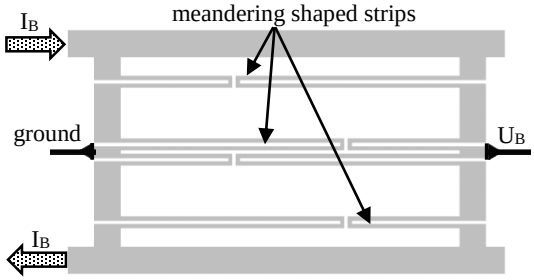

Figure 1a. Schematic of the THB-sensor

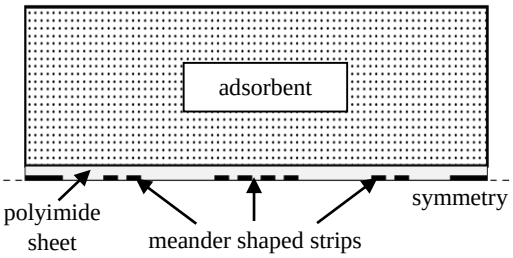

Figure 1b. Measurement setup in the simulation

1. Introduction

The measurement setup of the THB method is made up of the THB sensor which is clamped between two equivalent specimens. The whole set-up is located inside a chamber in which the vapor pressure of the working fluid can be precisely set. The sensor itself consists of a structured nickel film forming the conducting path between two polyimide sheets and is shown schematically in Figure 1a and Figure 1b. The eight meander shaped conductors are arranged symmetrically for an equal-resistance Wheatstone bridge. During measurement, the constant electric current I_B flows through the sensor and establishes an inhomogeneous temperature profile which changes the bridge voltage $U_B(t)$. The measured time-dependent bridge voltage is used to compute the thermal conductivity.

2. Equations for analytical evaluation

To derive an analytical evaluation, Hammerschmidt [1] made several simplifications to reduce computational complexity: the sensor hot strips are of infinite length and negligible thickness and the samples are considered infinitely large with homogenous material properties. With these assumptions the thermal conductivity can be calculated from

$$k_s = \frac{\alpha R_0^2 I_B^3}{32\pi L_s \left(\frac{\partial U_B(t)}{\partial(ln(t))}\right)_{max}} \qquad (1)$$

where α is the temperature dependent resistance coefficient of the structured nickel foil, R_0 is the reference resistance of nickel, I_B is the constant current, L_s is the length of one hot strip and $\left(\frac{\partial U_B(t)}{\partial(ln(t))}\right)_{max}$ is the maximum derivative of the bridge voltage with respect to the logarithm of time. Figure 2 shows the qualitative lapse of the

bridge voltage and its slope which is used for the evaluation.

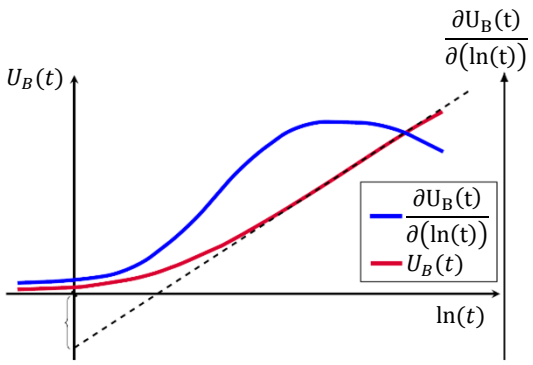

Figure 2. Qualitative lapse of the bridge voltage and its slope

3. Model equations in COMSOL

3.1 Constant Current equation

In order to simulate the bridge voltage signal of the sensor, the current conservation equation

$$\nabla(-\sigma\nabla V + J_e) = 0 \ , \qquad (2)$$

with

$$J_e = \frac{I_B}{d_{HS} \cdot b_{HS}} \qquad (3)$$

is used to specify the electric current I_B as well as the ground for measuring the bridge voltage, where σ is the linearized specific resistance, V is the electric potential J_e is the current density, d_{HS} is the thickness of the nickel film and b_{HS} is the width of the conducting path, where the current density is applied. In general the linearized specific resistance can be put in this form:

$$\sigma = \frac{1}{r_0\left(1 + \alpha\left(T - T_{ref}\right)\right)} \ . \qquad (4)$$

Here, r_0 represents the specific reference resistance and T_{ref} the reference temperature.

3.2 Heat Transfer

The heat transfer through the sensors polyimide foils is described with the energy equation

$$\nabla(k_{PI}\nabla T) = \rho_{PI} c_{p,PI} \frac{\partial T}{\partial t} \qquad (5)$$

where k_{PI} is the thermal conductivity, $c_{p,PI}$ the specific heat of polyimide and ρ_{PI} corresponds to the density.
To compute the heat transfer inside the porous specimen, the properties of the methanol vapor $\rho_v c_{p,v}$ and its velocity field u have to be considered in the energy equation

$$\nabla\left(k_{eff}\nabla T\right) + Q_s = \left(\rho c_p\right)_{eff} \frac{\partial T}{\partial t} + \rho_v c_{p,v} \boldsymbol{u} \cdot \nabla T \qquad (6)$$

Thereby, Q_s is a source term to take care of the adsorption heat (see [2]):

$$Q_s = \frac{h_{ad}}{c_{p,Adb}(X,T)} \frac{\partial X}{\partial t} \ . \qquad (7)$$

In this equation h_{ad} describes the adsorption enthalpy and X corresponds to the loading.
The effective specific heat, density and thermal conductivity in equation (5) are mixed material properties of activated carbon, methanol vapor and adsorbed methanol and are described with

$$k_{eff} = \varepsilon \cdot k_{Adb}(X,T) + (1-\varepsilon) \cdot k_v(T) \qquad (8)$$

$$\left(\rho c_p\right)_{eff} = \varepsilon \cdot \rho_{Adb}(X,T) c_{p,Adb}(X,T) + (1-\varepsilon) \cdot \rho_v(T) \cdot c_{p,v}(T) \qquad (9)$$

$$\rho_{Adb}(X,T) = \rho_{Adb,tr}(T) \cdot (1+X) \qquad (10)$$

$$c_{p,Adb}(X,T) = c_{p,Adb,tr}(T) + X \cdot c_{p,l}(T) \qquad (11)$$

The isotropic porosity $\boldsymbol{\varepsilon}$ is the ratio between the volume of voids and the total volume. It can be measured with mercury intrusion porosimetry

and takes a value of 0.39 for our specific specimen.

3.3 Species Transport

To simulate the mass transfer through the porous specimen, the species balance equation

$$\varepsilon \frac{\partial c}{\partial t} = R_i + \nabla(D_i \nabla c_i) \qquad (12)$$

is used. Here, the reaction term R_i describes the source term for the adsorption process:

$$R_i = \frac{\rho_{Adb,tr}(T)}{\varepsilon \cdot M} \frac{\partial X}{\partial t} \qquad (13)$$

Furthermore the species diffusivity

$$D_i = \bar{D}_{vis} + \bar{D}_{kn} \qquad (14)$$

is taken as the sum of the mean viscous diffusivity

$$\bar{D}_{vis} = \sum_{i=0}^{n} \left(\frac{p \cdot \xi_i \cdot d_{makro,i}^2}{32 \cdot \eta_v(T) \cdot \tau_{vis}} \right) \qquad (15)$$

and the mean Knudsen diffusivity

$$\bar{D}_{kn} = \sum_{i=0}^{n} \left(\frac{4}{3} \frac{\xi_i \cdot d_{makro,i}}{\tau_{kn}} \cdot \sqrt{\frac{RT}{2\pi M}} \right) \qquad (16)$$

In the equations above d_{makro} is the pore diameter distribution of the porous specimen, p is the vapor pressure, $\eta_v(T)$ is the temperature dependent dynamic viscosity, M is the molar mass of methanol, τ_{vis} and τ_{kn} are the tortuosities of the diffusivities and R is the universal gas constant. In Figure 3, the pore size distribution of the used activated carbon is shown.

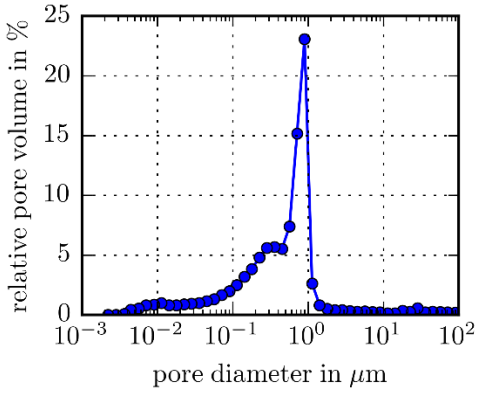

Figure 3. Pore size distribution of the activated carbon

3.4 Adsorption kinetics

The partial differential equation

$$\frac{\partial X}{\partial t} = \sum_{i=0}^{n} (\xi_i \cdot ksAp_i \cdot (X_{GG} - X_i)) \qquad (17)$$

is inserted to describe the adsorption kinetics. This equation is based on the linear driving force (LDF) model by using the time constant

$$ksAp_i = \frac{15 \cdot D_{Ad}}{r_{p,i}^2} \qquad (18)$$

to describe the adsorption process which depends on particle radius and diffusivity [3]. To consider the particle size distribution of the activated carbon raw material, a multistage model is used. In these equations ξ_i is the volumetric quantity of a particle radius, X_{GG} is the equilibrium load of methanol at certain pressure and temperature, X_i is the methanol loading of the particle, D_{Ad} is the adsorption diffusivity and r_p is the particle radius. A similar diffusion coefficient for all particles is assumed. Figure 4 shows the particle size distribution of the used activated carbon.

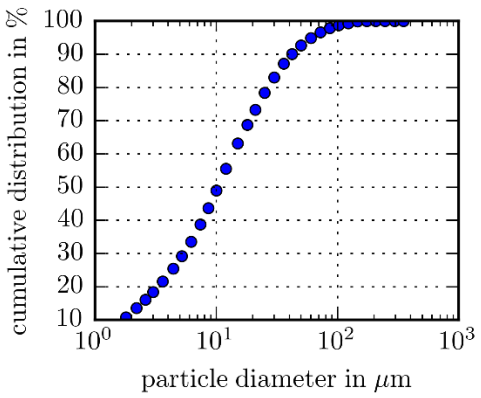

Figure 4. Particle size distribution of the used activated carbon

3.5 Boundary conditions

At the outer surfaces a zero flux in mass and heat transfer is assumed

$$-\boldsymbol{n} \cdot \boldsymbol{N_i} = 0 \quad (19)$$

$$-\boldsymbol{n} \cdot \boldsymbol{q} = 0 \quad (20)$$

and additionally there is a symmetry condition at the symmetry plane of the transient hot bridge sensor (see Fig. 1b).

3.6 Initial conditions

Specimen and sensor have the same initial temperature T_0, i.e., 303.15 K. The initial loading X_0 for the specimen is calculated with the initial temperature and pressure of the vapor.

4. Use of COMSOL Multiphysics

4.1 Geometry, Mesh and Physics

The geometry of the Sensor and specimen were generated in COMSOL 5.2 and are shown in Figure 5. To mesh the 40 µm wide and 2 µm thick nickel strips with the 22 mm wide and 10 mm thick specimen with a reasonable number of elements, the nickel foil is meshed with a mapped mesh, which is converted at the contact surface between nickel foil and specimen into a triangular mesh. The triangular mesh enables to mesh the specimen tetrahedral. To evaluate the required number of elements, a mesh study resulted in a mesh with 10000 domains, 23000 boundaries and 5200 edges to simulate the THB measurement with sufficient precision.

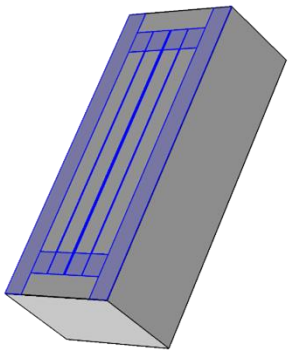

Figure 5. THB-sensor and porous specimen

For the implementation of the equations from chapter three, the COMSOL Physics: *Heat Transfer in Solid*, *Heat Transfer in porous Media*, *Transport dissolute species in porous Media* and *partial differential equation* were used.

4.2 Post-processing with use of Application Builder

COMSOL Application Builder is used to compute the load dependent thermal conductivity. Therefore the lapse of the bridge voltage and its slope are simulated and afterwards compared with the measured ones. Since not only the thermal conductivity of the specimen but also its density and heat capacity have an influence on the bridge voltage, the impacts of heat capacity and density were determined. The results show that both parameters only have an influence within the first seconds. Thus it is possible to adjust the thermal conductivity in the simulation until the lapse of the bridge voltage fits to the measured one. Thereby the lapse in the first seconds, where heat capacity and density have an influence, were not considered.

In order to perform a fast adjustment between the simulated and measured bridge voltage, the Nelder-Mead algorithm is implemented to minimize the sum of least squares between measured and simulated values of derivate bridge

voltage by altering the effective thermal conductivity of the specimen [4].

5. Results and Discussion

Measurements were performed in a vacuum chamber with controllable pressure of vapor to diversify the loading of the specimen. The first tests with the new measuring techniques were successfully performed with the working pair activated carbon and methanol. The computed effective thermal conductivity increases with rising methanol load due to the growing proportion of the thermal conductivity of the adsorbed phase. The computed value of the dry carbon complies to measurements with standard techniques. The Figure 6 presents the analytical and COMSOL evaluation of the load-dependent thermal conductivity.

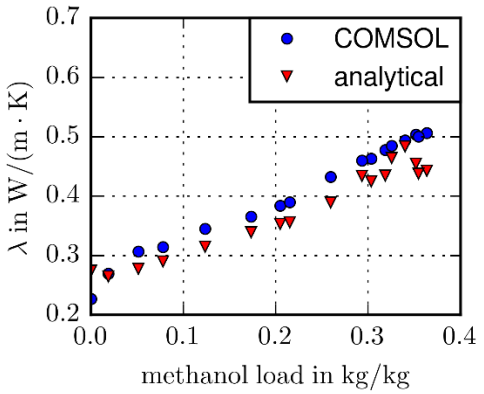

Figure 6. Thermal conductivity as a function of methanol load

Both evaluation methods show an increase of thermal conductivity with rising methanol load. In the complete measuring range the analytical values for thermal conductivity are lower than the COMSOL evaluated values, except at zero methanol loading. This can be attributed to the assumptions which were made for the simple analytical evaluation. In contrast to the new procedure using COMSOL, all thermal masses of the transient hot bridge sensor are not considered, internal thermal influences of the temperature profile are not considered and the local ad- and desorption is neglected.

Additionally, the analytical values show a non-continuous behavior at methanol loads higher 0.3 kg/kg. Due to low amperage, the maximum of the derivative of bridge voltage will not be reached and the determination of thermal conductivity is incorrect. Measurements at higher current levels would lead to methanol diffusion out of the specimen. In addition to this effect, the temperature profile would reach the boundaries of the specimen. Heat and mass transfer from the boundaries of the specimen to the test bench chamber is not considered in both evaluation methods.

6. Conclusions

It has been shown for the first time that it is possible to evaluate the load dependent thermal conductivity with a finite element model for a transient hot bridge sensor. The new technique extends the range of application of the transient hot bridge method and sheds light on the physics that influences the thermal conductivity of porous media.

7. References

[1] U. Hammerschmidt and V. Meier, New Transient Hot-Bridge Sensor to Measure Thermal Conductivity, Thermal Diffusivity, and Volumetric Specific Heat, International Journal of Thermophysics 27.3, S. 840–865 (2006)

[2] Schnabel, L. (2009): Experimentelle und numerische Untersuchung der Adsorptionskinetik von Wasser an Adsorbens-Metallverbund-strukturen. Berlin: Technische Universität Berlin.

[3] Kast, W. (1988): Adsorption aus der Gasphase, Ingenieurwissenschaftliche Grund-lagen und technische Verfahren. VCH Verlagsgesellschaft Weinheim – Basel – New York

[4] Nelder, J. A. und Mead, R. (1965): A simplex method for function minimization. The Computer Journal 7, S. 308–313.

8. Acknowledgements

This research was supported by the German Federal Ministry of Education and Research, research grant 03FH023PX4 (OptiSorp).
Support from Linseis Messgeräte GmbH during the conduct of this work was greatly appreciated.

9. Nomenclature

D_{Ad}	$\frac{m^2}{s}$	Adsorption diffusivity
D_i	$\frac{m^2}{s}$	Diffusion coefficient
$\overline{D}_{kn}$	$\frac{m^2}{s}$	Mean Knudsen diffusivity
$\overline{D}_{vis}$	$\frac{m^2}{s}$	Mean viscous diffusivity
I_B	A	Current of Wheatstone Bridge
J_e	$\frac{A}{m^2}$	Current density
L_s	m	Length of Transient Hot Strip
M	$\frac{kg}{mol}$	Molar Mass of fluid
Q_s	$\frac{W}{m^3}$	Heat source term
Q_{Ads}	$\frac{W}{m^3}$	Adsorption source in energy balance
R	$\frac{J}{mol \cdot K}$	Universal gas constant
R_0	Ω	Reference resistance of nickel
R_i	$\frac{mol}{m^3 \cdot s}$	Mass source term
T	K	Temperature
T_{ref}	K	Reference temperature
U_B	V	Bridge Voltage
V	V	Electric potential
X	$\frac{kg}{kg}$	Load of adsorbate
X_{GG}	$\frac{kg}{kg}$	Equilibrium load of adsorbate
b_{HS}	m	Width of conducting path
c	$\frac{mol}{m^3}$	Concentration
c_p	$\frac{J}{kg \cdot K}$	Specific heat capacity
$c_{p,eff}$	$\frac{J}{kg \cdot K}$	Effective specific heat capacity
$c_{p,Adb}$	$\frac{J}{kg \cdot K}$	Specific heat capacity of the adsorbent
$c_{p,Adb,tr}$	$\frac{J}{kg \cdot K}$	Specific heat capacity of adsorbent without adsorbed fluid
$c_{p,l}$	$\frac{J}{kg \cdot K}$	Specific heat capacity of liquid fluid
$c_{p,PI}$	$\frac{J}{kg \cdot K}$	Specific heat capacity of Polyimid
$c_{p,v}$	$\frac{J}{kg \cdot K}$	Specific heat capacity of fluid vapor
d_{HS}	m	Thickness of nickel film
d_{makro}	m	Pore diameter of adsorbent
h_{ad}	$\frac{J}{kg}$	Adsorption enthalpy
k	$\frac{W}{m \cdot K}$	Thermal conductivity
k_{Adb}	$\frac{W}{m \cdot K}$	Thermal conductivity of the adsorbent
k_{eff}	$\frac{W}{m \cdot K}$	Effective thermal conductivity
λ_s	$\frac{W}{m \cdot K}$	Analytical evaluated Thermal conductivity
k_v	$\frac{W}{m \cdot K}$	Thermal conductivity of vapor
$ksAp$	$\frac{1}{s}$	Adsorption time constant
p	Pa	Pressure
r_0	$\Omega \cdot m$	Specific reference resistance
r_p	m	Particle radius
t	s	Time
u	$\frac{m}{s}$	Velocity field for convection term
α	$\frac{1}{K}$	Temperature dependent resistance coefficient
ε	$-$	Porosity of adsorbent
η_v	$Pa \cdot s$	Dynamic viscosity of fluid vapor
ξ	$-$	Relative pore volume
ρ	$\frac{kg}{m^3}$	Density
ρ_{Adb}	$\frac{kg}{m^3}$	Density of adsorbent
$\rho_{Adb,tr}$	$\frac{kg}{m^3}$	Density of adsorbent without adsorbed fluid
ρ_{eff}	$\frac{kg}{m^3}$	Effective Density
ρ_{PI}	$\frac{kg}{m^3}$	Density of Polyimid
ρ_v	$\frac{kg}{m^3}$	Density of vapor

σ	$\frac{s}{m}$	Linearized specific resistance
τ_{vis}	$-$	Viscous tortuosity of adsorbent
τ_{kn}	$-$	Knudsen tortuosity of adsorbent